GT2024-128208

FILM COOLING EFFECTIVENESS MEASUREMENTS ON A CMC-SIMULATED FLAT PLATE

Douglas Thurman
NASA Glenn Research Center
Cleveland, OH

Philip Poinsatte
NASA Glenn Research Center
Cleveland, OH

ABSTRACT

Ceramic matrix composites (CMC) are high temperature materials that can allow higher operating turbomachinery engine temperatures with less coolant required. One method of fabricating ceramic matrix composites is by weaving fibers into the shape of an airfoil. Generally, CMC fiber tows are assembled with various weave patterns, but this uneven surface could introduce aerodynamic losses, and it will be necessary to determine the best film cooling hole arrangement for minimal thermal engine efficiency loss. As part of an effort to assess the impact of geometric constraints of CMC implementation relative to metallic high pressure turbine blades, an experimental study was performed to investigate the effect of film cooling on a CMC-like surface roughened flat plate. Film cooling effectiveness measurements were acquired on a large-scale surface with a ceramic matrix composite weave pattern and on a smooth surface for comparison. A single row and a 2-row cooling hole arrangement were investigated with different hole sizes. Infrared thermography data was acquired at several Reynolds numbers and blowing ratios. Results showed that the effect on span averaged film cooling effectiveness was small between a weave surface pattern and a smooth surface, while hole spacing dependence had a much stronger effect.

Keywords: Ceramic matrix composites, film cooling

NOMENCLATURE

BR	blowing ratio
D	hole diameter
IR	infrared
P	spanwise hole spacing
Ra	Arithmetic average roughness
Re	Reynolds number
ρ	density
S	hole spacing between rows
T	temperature
U	velocity
η	film cooling effectiveness
∞	freestream

1. INTRODUCTION

Ceramic matrix composites (CMC) are becoming more widely used in aerospace applications. Their capability for high temperature and lighter weight makes CMC's appealing for the hot temperatures seen in modern gas turbine engines. As a result, less cooling flow is necessary for hot gas path components, thus increasing overall engine efficiency.

While CMC's can withstand higher temperatures, turbine engine temperatures are higher than CMC material limits, and some form of cooling will still be required. There are also various techniques to fabricate CMC airfoils. One method involves weaving the high strength fibers. This weave produces an irregular rough surface compared to smooth polished metal used to fabricate turbine blades. Krishna and Ricklick [1] investigated the effect of jet impingement on a simulated CMC surface; their results showed negligible changes in Nusselt number compared to a smooth surface. Film cooling of combustor liners and high pressure turbine blades and vanes is conventionally used to provide a thin layer of cooler air that is bled from the compressor of the engine to help protect the metal surface from the extreme freestream temperatures. The placement of holes on CMC airfoils however may be affected by the properties of the material, and there is limited documentation in open literature on the effects of cooling holes on ceramic materials. Wilkins et al [2] presented analytical results of the effects of a weaved CMC surface on film cooling, as well as the effect on the boundary layer [3]. Edelson et al. [4] showed film effectiveness measurements on a weaved CMC topology along the internal channel, external surface, and along both surfaces with a 7-7-7 hole, indicating that the weave surface increases mixing between the coolant and freestream flows compared to a smooth surface. Wilkins et al. [5] reported data that showed some CMC surface effects on film cooling with shaped holes. Zhao et al. [6] investigated drilled and preformed film cooling holes on braided CMC plates; they showed that preformed film cooling holes provided better performance in controlling the thermal gradient around the holes compared to drilled film cooling holes. Optimization of the location of film cooling holes is typically done using analytical codes. Boyle et al. [7, 8]

explored issues associated with replacing metallic vanes in a high pressure turbine with two-dimensional weaved CMC's; it was noted that film cooling and trailing edge ejection may be required to avoid excessive temperature gradients. Smith et al. [9] performed experiments on sample CMC's with film cooling holes showing local strain and stress effects of straight and angled film cooling holes with a fixed pitch and multiple rows. Mehta et al [10] performed an analytical study with multi-hole film cooling with woven ceramic wall panels of a combustor liner that showed better film cooling effectiveness with higher effective conductance and reduced thermal stresses. El-Gabry and Kiminski [11] discussed heat transfer distribution on roughened surfaces with an array of impinging jets and found the lowest decrease in spanwise averaged Nusselt number with film cooling jets impinging on a roughened surface compared to a smooth surface.

This paper aims to show the effects of a weaved CMC surface with various film cooling hole patterns and assess any differences relative to a smooth surface with similar film cooling configurations. The intention is to show that relative to a smooth surface, a CMC patterned surface would, at least, demonstrate no film cooling detriment and possibly provide an improvement in film effectiveness; specifically, would the roughened patterned surface provide any flow disturbance below the cooling jet to keep if better attached to an airfoil surface. The surface features investigated in this study are representative of a typical weaved CMC surface without an environmental barrier coating (EBC). EBC's are typically applied to turbine airfoils to protect the surface from the extreme temperatures and environments containing sand and humidity experienced in the engine; they could tend to smooth out any roughness in a weaved surface.

2. MATERIALS AND METHODS

The NASA Engine Research Building SW-6 Fundamental Film Cooling Facility, shown in Figure 1, consists of an aluminum bellmouth, flow conditioning screens, and a square acrylic section 207 mm x 207 mm (8.15 inch x 8.15 inch) wide with 19.05 mm (0.75 inch) thick walls. The tunnel was connected to a blower fan downstream that pulled room air through. The test section consisted of a floor piece fabricated from ABS*plus* thermoplastic in a 3-D printer, in which 152.4 mm (six-inch) square interchangeable acrylic and ABS test plates could be used. A FLIR infrared camera was mounted above the test section and viewed the removeable test plates through a zinc selenide window. A heated air supply using three 75W inline

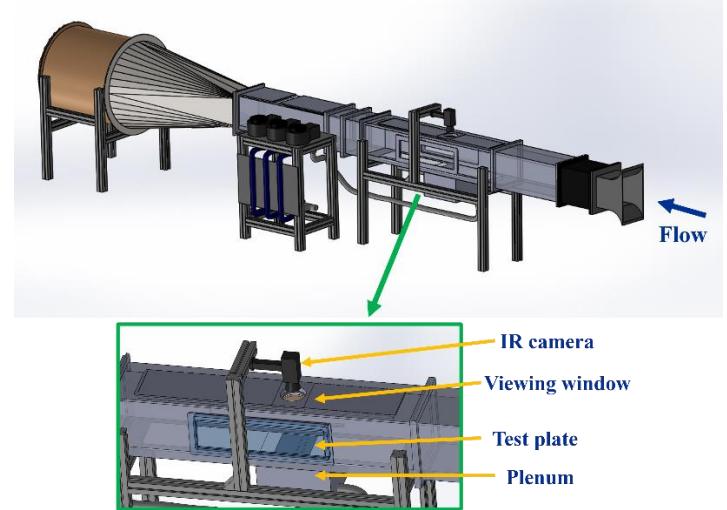heaters fed the plenum beneath the test plates.

FIGURE 1: FILM COOLING TUNNEL WITH CLOSEUP OF TEST PLATE AND PLENUM

In order to fabricate a CMC-like weave pattern on the surface, a 3-D scan of a sample weaved CMC coupon with no EBC coating was performed, and a gray-scaled bitmap image was exported. Figure 2a shows the CMC coupon and the resulting bitmap generated. For this CMC coupon, the dominant direction of the weave is horizontal in the figure. The 50.8-mm x 50.8-mm (2-inch x 2-inch) coupon had a weave tow (group of fibers) width of approximately 1 mm, which also is the same diameter of a typical film cooling hole. Test plates were scaled to match the available flow rates in the tunnel based on hole diameter, resulting in Reynolds numbers similar to the suction side of a turbine blade using a single row of film cooling holes and near half that for two rows of film cooling holes. An average surface roughness of the coupon was measured to be Ra_{avg}=28 μm, with the test plate roughness scaled similarly and measured to be roughly Ra_{avg}=141 μm. Using the gray-scaled image, a laser etching machine was then used to etch the weave pattern onto a 6.35 mm (0.25 inch) thick acrylic sheet, with the depth of the surface features based on the gray scale of the image (darker regions had higher laser power, thus deeper etch). Typically nine passes were required to produce the desired depth of the weave that scaled to the original CMC sample. Additionally, a new computer aided design (CAD) program was developed to create the weaved texture on the multirow plates in order to fabricate test plates with a 3D printer using ABS material. This method was quicker and more consistent for fabrication.

Film cooling holes were drilled into the plates inclined at 30 degrees from the horizontal surface, with diameter *D* varying from 4.5 mm to 12.7 mm (0.177 inch to 0.5 inch), hole spacing *P/D* from 2 to 5, and *L/D* of approximately 2.6. Both single-row and two-staggered-row holes were tested, allowing for periodic flow and boundary conditions. Images of the two types of test plates are shown in Figure 2b. Smooth plates matching the hole patterns were also fabricated for comparison with the ABS and

laser etched acrylic plates. Table 1 shows the heat transfer cases that were tested.

A PC-based data acquisition system was used to acquire data from pressure transducers and thermocouples. The tunnel flow rate was measured from a total pressure probe placed upstream of the test section and static pressure taps located on the sidewalls. Freestream temperature was measured with a thermocouple located upstream of the holes near the total pressure probe. Tunnel flow ranged from 9.14 - 18.28 m/s (30 – 60 ft/s) at ambient conditions, providing Reynolds numbers based on hole diameter and freestream velocity of 3500 to 19,000. Freestream turbulence was measured with hot wire anemometry to be less than 1% at the inlet to the test section, and a boundary layer thickness measured around 20.32 mm (0.8 inch).

The injection flow was provided by blowing pressurized air through a flow meter and into a plenum attached to the underside of the test section floor plate. The injection flow conditions were measured with static pressure taps and thermocouples inside the plenum. In previous film cooling tests with this tunnel [12], a cooled injected air was used, in which the injected air was cooled by passing through copper tubing that was coiled inside an ice water tank, which provided a temperature difference of nominally 1.67 °C (35 °F). However this test employed a heated jet which provided a larger temperature difference was desired, so the injection air was heated using three 750 W in-line electrical pipe heaters. This provided a temperature difference of approximately 23.9 °C (75 °F). Little difference was found between the heated and cooled jet.
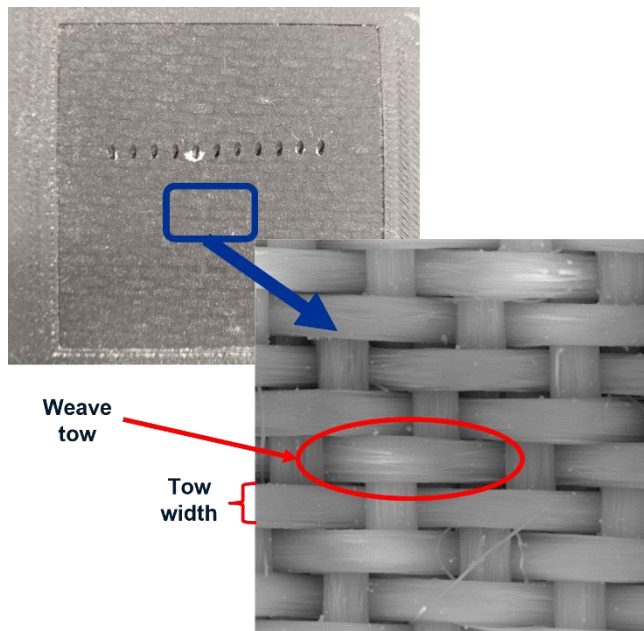

FIGURE 2A: WEAVED CMC SAMPLE COUPON WITH ZOOMED IN 3-D SCAN OF WEAVE PATTERN

FIGURE 2B: SAMPLE TEST PLATES: D=0.5 INCH WITH STREAMWISE (0 DEG) WEAVE (TOP), SPANWISE (90 DEG) WEAVE (MIDDLE), D=0.177 INCH WITH SPANWISE (90 DEG) WEAVE (BOTTOM)

CMC flat plate heat transfer cases						
Surface	D (inch)	Hole P/D	Row S/D	# holes	Re_D	scale
spanwise (90°) weave	0.5	2		3	7500; 11000; 14500	12.7
smooth	0.5	3		3	7500; 11000; 14500	12.7
streamwise (0°) weave	0.5	3		3	7500; 11000; 14500	12.7
spanwise (90°) weave	0.5	3		3	7500; 11000; 14500	12.7
spanwise (90°) weave	0.5	4		3	7500; 11000; 14500	12.7
smooth	0.177	2	4	13 (7 top, 6 bottom)	3500; 4500; 5500	4.53
spanwise (90°) weave	0.177	2	4	13 (7 top, 6 bottom)	3500; 4500; 5500	4.53
smooth	0.177	3	4	13 (7 top, 6 bottom)	3500; 4500; 5500	4.53
spanwise (90°) weave	0.177	3	4	13 (7 top, 6 bottom)	3500; 4500; 5500	4.53
smooth	0.177	4	4	13 (7 top, 6 bottom)	3500; 4500; 5500	4.53
spanwise (90°) weave	0.177	4	4	13 (7 top, 6 bottom)	3500; 4500; 5500	4.53
smooth	0.177	5	4	11 (5 top, 6 bottom)	3500; 4500; 5500	4.53
spanwise (90°) weave	0.177	5	4	11 (5 top, 6 bottom)	3500; 4500; 5500	4.53

TABLE 1: EXPERIMENTAL CASES

Data at blowing ratios ranging from 0.5 to 3 were acquired, where

$$BR = \frac{(\rho U)_{injection}}{(\rho U)_{freestream}} \qquad (1)$$

An uncertainty analysis performed on the effectiveness measurements showed the data to be nominally within 5%.

3. RESULTS AND DISCUSSION

Surface contour plots of film cooling effectiveness was calculated for both smooth and weaved surfaces over different tunnel flow rates and film cooling blowing ratios. Film cooling effectiveness is defined as

$$\eta = \frac{(T_\infty - T_{IRsurface})}{(T_\infty - T_{plenum})} \approx \frac{(T_{IRupstrm} - T_{IRsurface})}{(T_{IRupstrm} - T_{plenum})} \qquad (2)$$

where T_∞ is the temperature of the freestream, $T_{IRupstrm}$ is the temperature of the infrared surface image near an upstream surface thermocouple, $T_{IRsurface}$ is the temperature of the infrared image, and T_{plenum} is the temperature from a thermocouple placed in the center of the quiescent plenum. Either the air temperature or the IR upstream surface temperature can be used to calculate the effectiveness. While the airstream turbulence was relatively low, the air thermocouple temperature could fluctuate ~+/-0.5 degrees and would have to be averaged appropriately depending on the specific test velocities. The upstream surface temperature however closely matched the average airstream thermocouple that was located above it. Thus the data was reduced using the IR temperature at the upstream location to facilitate data reduction and improve uncertainty by avoiding the need to average and image time-match the airstream thermocouple.

A span-averaged effectiveness over one-pitch (+/- half pitch along the center hole) was used to compare cases. Initial studies included acrylic flat plates with a single row of three film cooling holes with 12.7 mm (0.5-inch) diameter to allow for higher Reynolds number flows. Later studies included ABS flat plates with two staggered rows of holes with 4.5 mm (0.177-inch) diameter.

To determine the effect of weave orientation, three plates with single row holes at P/D=3, Re=11,000, and BR=2 were used: one with a smooth surface, one with the dominant weave texture in the streamwise direction (0°, same direction as the freestream flow), and the other with the dominant weave texture in the spanwise direction (90°, perpendicular to the freestream flow). Figure 3a shows contour plots of effectiveness values for the streamwise (0°) weave and the spanwise (90°) weave, and Figure 3b shows the spanwise-averaged film cooling effectiveness values for the center hole of the plate for each of the three plates. Note that the leading edge of the hole is at x/D=0, and the center hole is at y/D=0. This data generally compared favorably to previously published data from the same facility [12]. However, the high values seen around the hole in Figure 3a are probably due to conduction from the backside of the test plate and through the hole rather than actual protection from the coolant film layer. This near hole conduction was especially prevalent due to the thin substrate employed in these current tests.

While the streamwise (0°) weave and spanwise (90°) weave contour plots appear fairly similar, the spanwise (90°) weave tends to spread out the coolant slightly more downstream of the holes. There is also noticeable spreading near the hole's leading edge and along the edge of each weave downstream of the holes. Figure 3b shows the one-pitch centerline span-averaged film effectiveness as a function of distance downstream of the film hole. The better performance of the spanwise (90°) weave pattern is clearly seen; the spanwise weave provides roughly 25% higher effectiveness than the streamwise weave. For this reason, the spanwise (90°) weave was used for all subsequent cases.

Figure 4 shows the Reynolds number effect on film cooling effectiveness for a typical data set. Little variation in Reynolds number is seen for the spanwise weave surface at P/D=3 and BR=2, so the following single row plate results will be for Re=11,000. Figure 5 shows film effectiveness contour plots of the different hole spacing at the lowest blowing ratio of 0.5 and at the highest blowing ratio of 3. Increased blowing ratio results in coolant blowoff and thus lower effectiveness downstream of the holes. For the narrow pitch P/D=2 cases, the overall downstream effectiveness is higher relative to the wider pitch cases. Additionally, the narrow pitch case shows some jet coalescing and reattachment downstream which is possibly due to the tunnel setup; thus, the interpretation of the effectiveness data for this case has some concern. The weaved surfaces tend to have a slightly wider coverage of coolant downstream of the holes compared to the smooth surface.
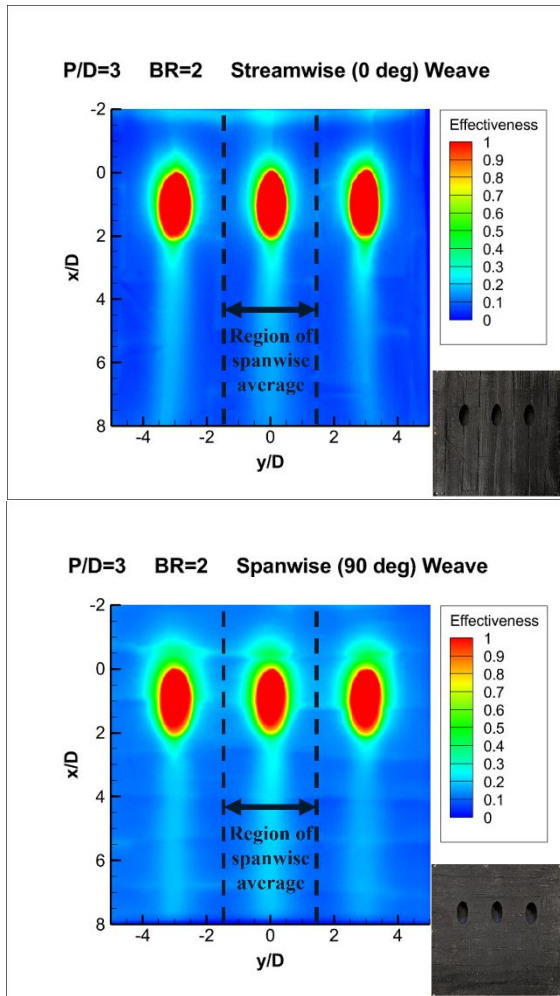
FIGURE 3A: SURFACE FILM COOLING EFFECTIVENESS CONTOUR PLOTS FOR STREAMWISE (0 DEG) WEAVE (TOP) AND SPANWISE (90 DEG) WEAVE (BOTTOM) SURFACES WITH P/D=3, RE=11,000, AND BR=2
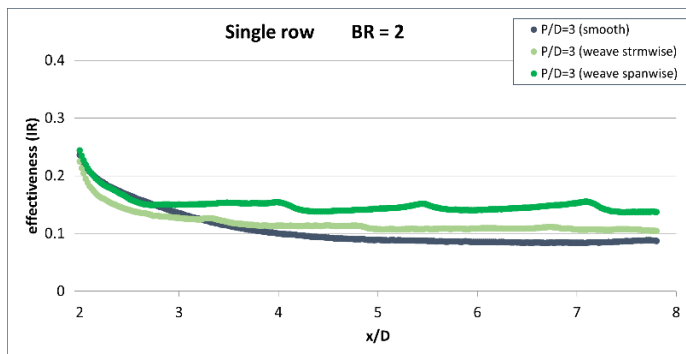

FIGURE 3B: SPAN-AVERAGED FILM COOLING EFFECTIVENESS FOR SMOOTH, STREAMWISE (0 DEG) WEAVE, AND SPANWISE (90 DEG) WEAVE SURFACES WITH SINGLE ROW PLATE, P/D=3, RE=11,000, AND BR=2 (X/D=0 AT LEADING EDGE OF HOLE)

To better compare the effects of surface roughness, Figure 6 shows the effect of blowing ratio on span averaged effectiveness for the smooth and weaved plates with different hole spacing. For all the cases, increasing blowing ratio results in decreasing effectiveness. In Figure 6a, the downstream effectiveness for a smooth plate is seen to decrease from 0.17 for BR=0.5, to 0.11 for BR=1, to 0.08 for BR=2 and 3; values for BR=2 and 3 are nearly identical which indicates nearly complete jet blowoff for each case. Comparing smooth P/D=3 (Figure 6a) to the textured plate P/D=3 (Figure 6c), the weaved surface effectiveness also decreases with increasing blowing ratio and approaches the lowest smooth plate value at BR=3, but the weave surface value for BR=2 shows improvement over the smooth case. This single row data seems to indicate surface texture may provide a beneficial effect in keeping the jet better attached to the surface by altering the turbulence and any secondary flow features beneath the jet.

In Figure 6b with the weaved plate and P/D=2, effectiveness decreases moving from BR=0.5 to 1, and then increases moving from BR=2 to 3. As blowing ratio approaches 2 and 3, it appears that the jets begin to liftoff, but further downstream the outer jets merge together. It is unclear if the jets are being entrained toward each other or perhaps pushed inward by the freestream flow, potentially biasing these results. This coalescing of the jets shows significantly increased span averaged effectiveness values, as seen in the contour plot of Figure 5a, which is counterintuitive to usual wider hole pitch film cooling effectiveness results. Additional holes at this spacing may have reduced this squeezing effect on the center holes and would have allowed the center jets to flow straighter. These data plots are included here for completeness. For the weave P/D=3 and P/D=4 cases (Figures 6c and 6d), the holes are far enough apart that there is little interaction between the jets. The P/D=3 data shows an improvement of effectiveness relative to the smooth surface data. In Figure 6d with P/D=4, the effectiveness is fairly similar to the smooth plate, with the bumps in the data resulting from the increased effectiveness along the edge of each weave. Again this single row data seems to indicate surface texture may provide a beneficial effect in keeping the jet better attached to the surface allowing wider hole spacing and perhaps less overall film flow rate. Note that the data for BR=3 is cut off after x/D=6.2 due to camera view surface obstruction.
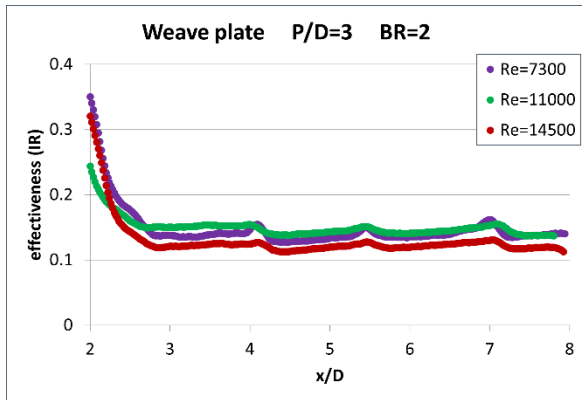
FIGURE 4: REYNOLDS NUMBER EFFECT ON SINGLE ROW PLATE WITH SPANWISE (90 DEG) WEAVE SURFACE, P/D=3, AND BR=2
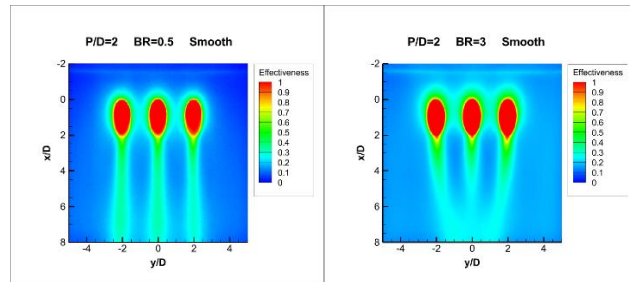

FIGURE 5A: EFFECTIVENESS CONTOUR PLOTS FOR SMOOTH PLATE: P/D=2, RE=11,000, BR=0.5 (LEFT), BR=3 (RIGHT)

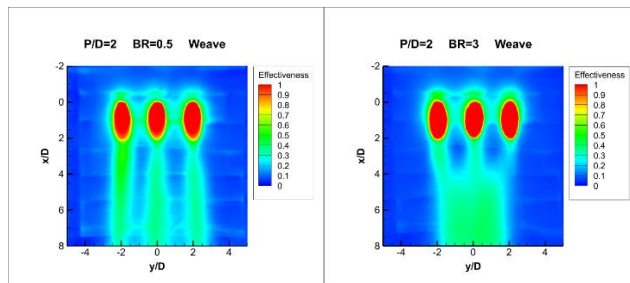**FIGURE 5B:** EFFECTIVENESS CONTOUR PLOTS FOR SPANWISE (90 DEG) WEAVE PLATE: P/D=2, RE=11,000, BR=0.5 (LEFT), BR=3 (RIGHT)
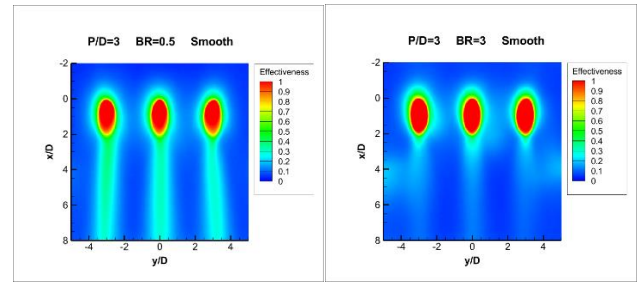

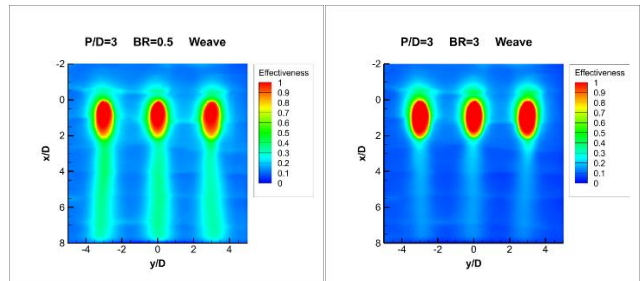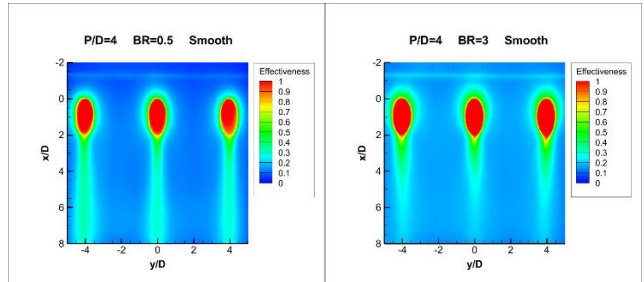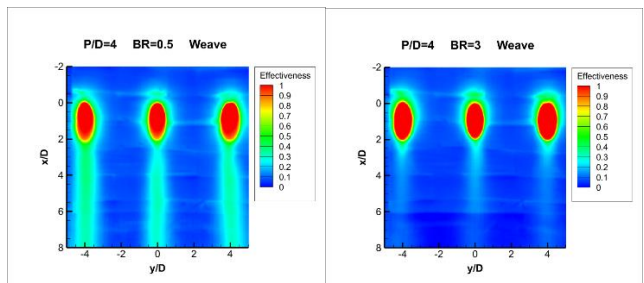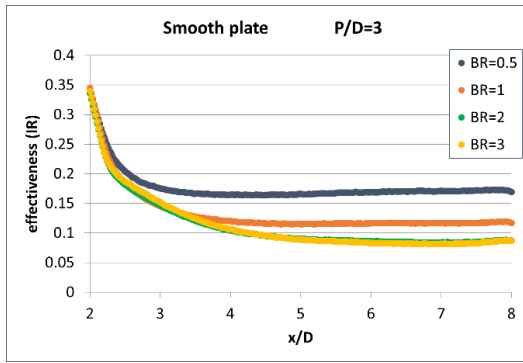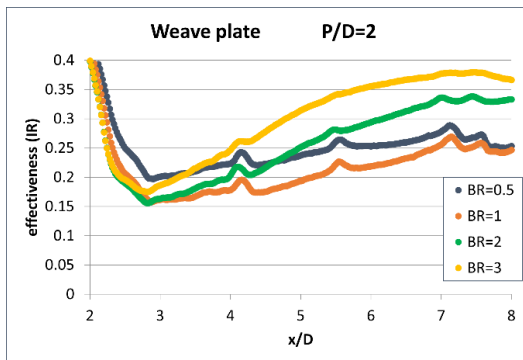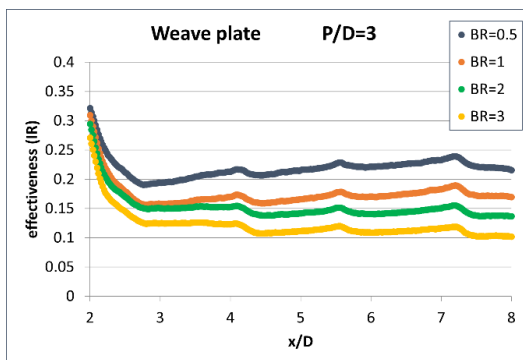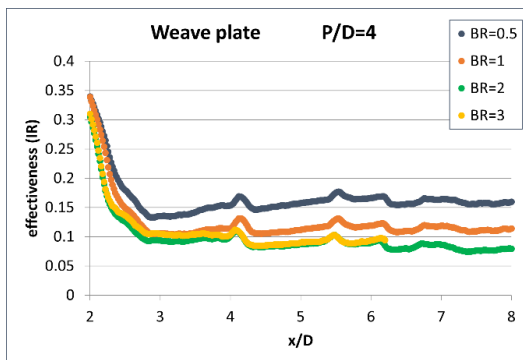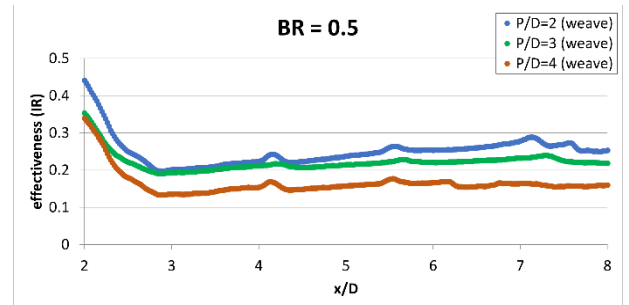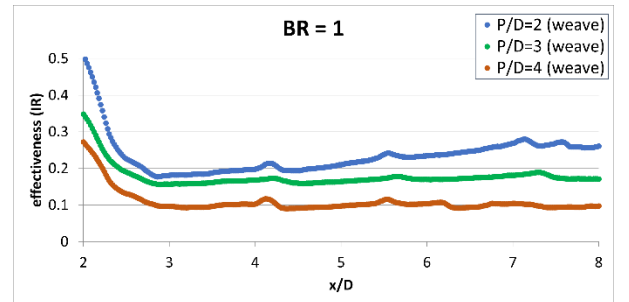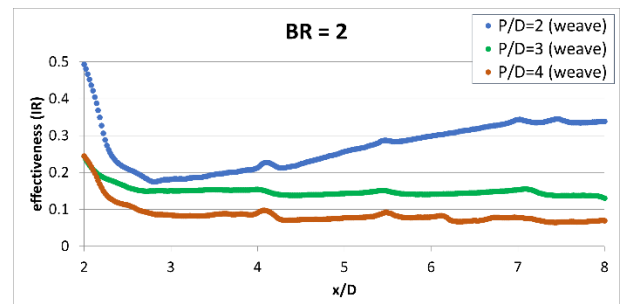**FIGURE 5C:** EFFECTIVENESS CONTOUR PLOTS FOR SMOOTH PLATE: P/D=3, RE=11,000, BR=0.5 (LEFT), BR=3 (RIGHT)

FIGURE 5D: EFFECTIVENESS CONTOUR PLOTS FOR SPANWISE (90 DEG) WEAVE PLATE: P/D=3, RE=11,000, BR=0.5 (LEFT), BR=3 (RIGHT)

FIGURE 5E: EFFECTIVENESS CONTOUR PLOTS FOR SMOOTH PLATE: P/D=4, RE=11,000, BR=0.5 (LEFT), BR=3 (RIGHT)

FIGURE 5F: EFFECTIVENESS CONTOUR PLOTS FOR SPANWISE (90 DEG) WEAVE PLATE: P/D=4, RE=11,000, BR=0.5 (LEFT), BR=3 (RIGHT)

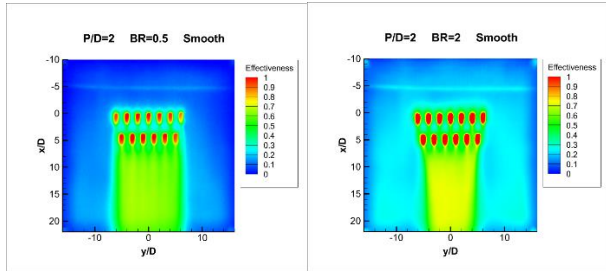**FIGURE 6:** SPAN-AVERAGED EFFECTIVENESS AT RE=11,000 SHOWING EFFECT OF BLOWING RATIO

FIGURE 7: SPAN-AVERAGED EFFECTIVENESS AT RE=11,000 SHOWING EFFECT OF HOLE SPACING

The span-averaged effectiveness in Figure 7 further shows the effect of hole spacing on the single row of holes at each blowing ratio for the weaved plates. In general, effectiveness decreases with larger hole spacing and increased blowing ratio. As seen in Figure 5, coverage behind each hole also tends to decrease with larger hole spacing and blowing ratio, but the
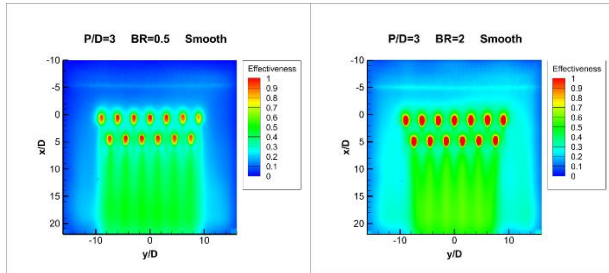
weaved surface tends to have slightly more coverage than for a smooth surface. At BR=3, jet blowoff results in about the same low effectiveness for P/D=3 and 4. Note that the data for BR=3 is cut off after x/D=6.2 due to camera view surface obstruction. Not surprisingly, the closer spaced holes have a higher effectiveness. The effect of P/D=2 however is potentially exaggerated at the high blowing ratios BR=2 and 3 due to the squeezing of the blowoff jets by the mainstream flow, creating a region with high effectiveness values as seen in Figure 5b. While the span averaged effectiveness calculated over one hole pitch (center hole), the overall effective area of cooling is reduced as will be seen below in multi-row data.
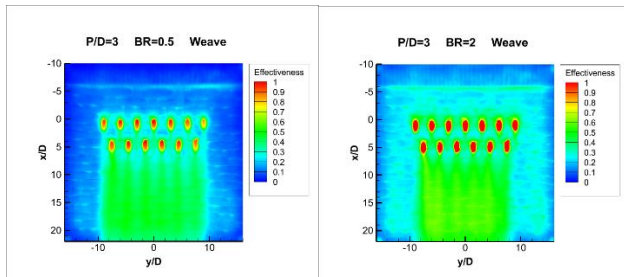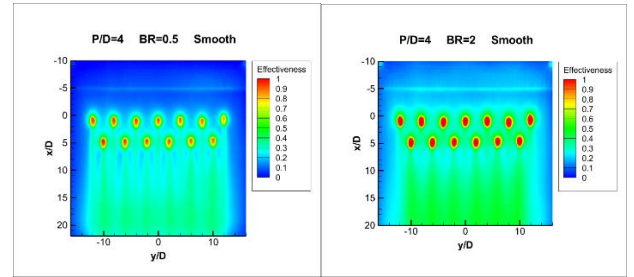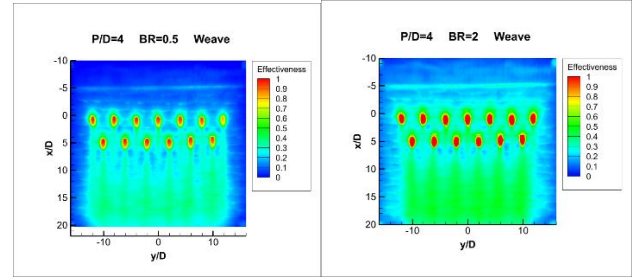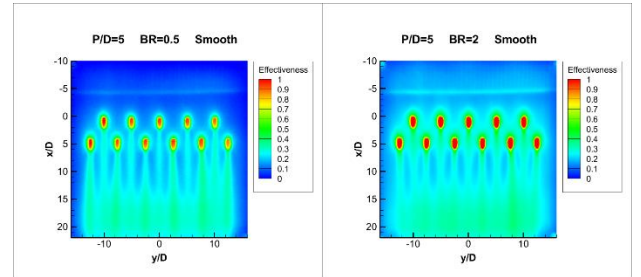
A)

B)

C)

D)

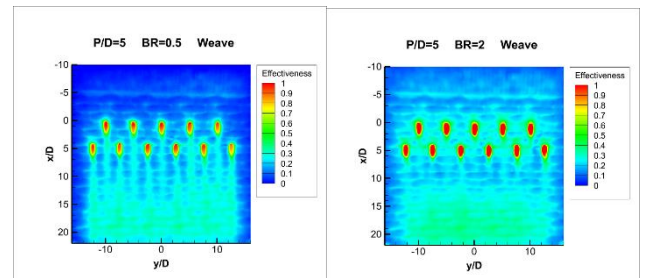E)

F)

G)

H)

FIGURE 8: SURFACE FILM COOLING EFFECTIVENESS CONTOUR PLOTS FOR SMOOTH AND SPANWISE (90 DEG) WEAVED SURFACES WITH P/D=4, RE=5500, AND BR=1

Typically a film cooled blade has multiple rows of film cooling holes, so a two-row staggered hole configuration was also investigated. These plates were additively manufactured from ABS plastic with and without the weave texture; a representative weaved plate is shown in Figure 2. Due to flow limitations of the facility, the highest Reynolds number that could be run was 5500. Little difference was observed between the three Reynolds flow cases that were run, and all showed similar trends, thus only the Re=5500 cases are presented. Figure 8 shows surface film cooling effectiveness contour plots for smooth and spanwise (90 deg) weaved surfaces at Re=5500. The effects of surface roughness are not as evident as the contour plots seem quite similar, although the distinct weave patterns are visible for the weaved plate. As with the single row cases, the same squeezing of the blowoff jets can be seen at BR=2. So while the film effectiveness is high behind the P/D=2 rows the total area of coverage is lessened. In general, there is not much difference between the smooth and weaved surfaces as the second row of holes adds more mixing of the flow and overwhelms the effect of the surface roughness. As hole spacing increases, the weave surface appears to be less effective just downstream of the holes.

Figure 9 shows the span-averaged effectiveness along the center hole. The blocked out regions are the hole row locations x/D=0 to 3 and x/D=5 to 7, with variations due to backside conduction near the hole. As expected, effectiveness decreases with increasing hole spacing. The two-row data may show in some cases small improvement with surface texture over smooth case, but the effect is less pronounced than in the single row data. The interaction of multiple rows seems to lessen the benefit of surface texture to jet attachment. Interestingly the P/D=2 case shows the only significant improvement, e.g., the weaved surface shows up to 20% increase in effectiveness near the holes at x/D=9. The other hole spacings show no or only very marginal improvement.
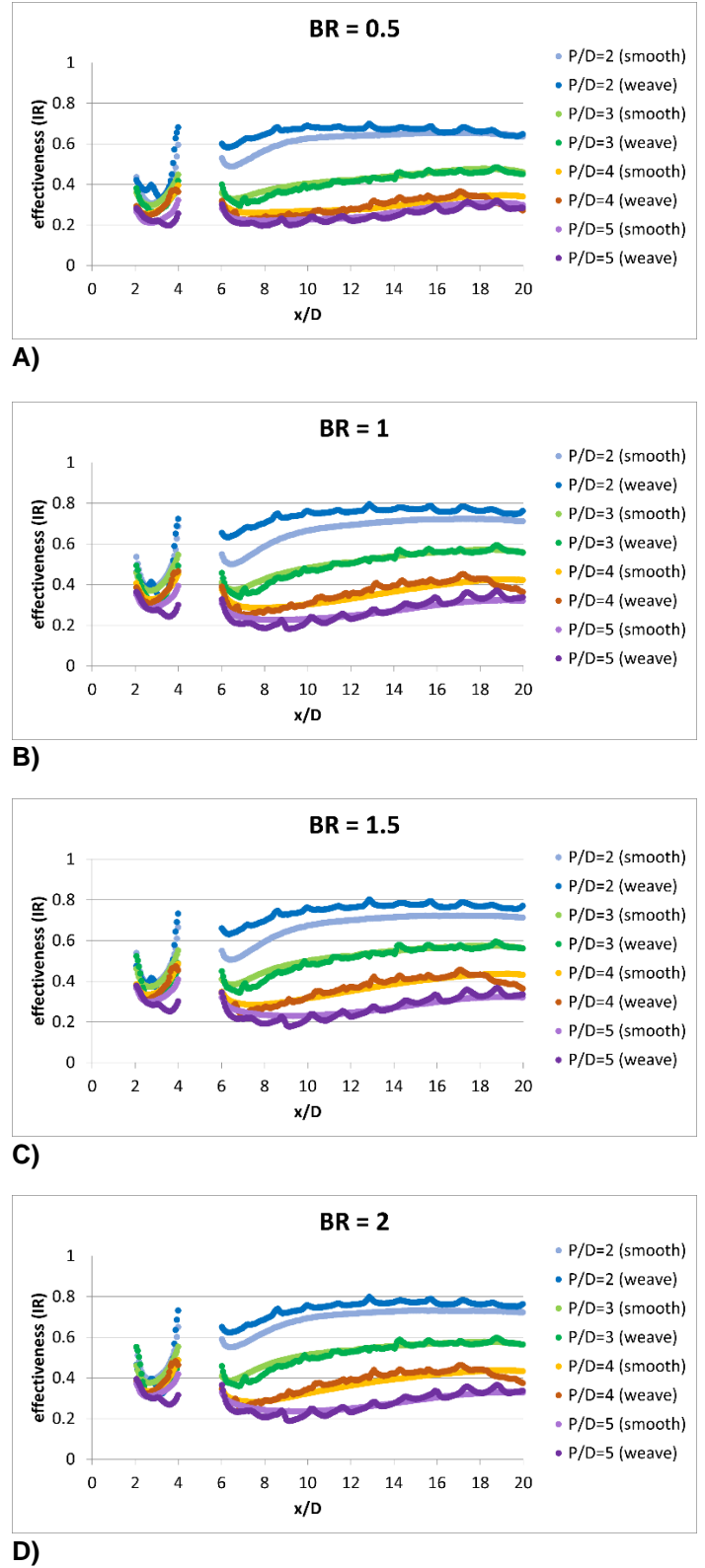

FIGURE 9: SPAN-AVERAGED EFFECTIVENESS FOR 2-ROW COOLING AT RE=5500

4. CONCLUSION

An experimental study was performed to investigate the effect of film cooling on a CMC-like surface roughened flat plate with the aim to provide a comparison of the effects of a smooth versus weaved CMC surface with various film cooling hole patterns. Film cooling effectiveness was measured on a single row and a two-row cooling hole arrangement using infrared thermography at several flow rates and blowing ratios. The single row span-averaged effectiveness results showed that the roughened weave surface pattern certainly was not detrimental to film cooling and, in some cases, helped somewhat with keeping the coolant jet from blowing off at higher blowing ratios. However, for the two-row configuration, little effectiveness difference was seen between the weaved and smooth surfaces. Hole spacing had a much stronger effect on the span averaged data although the film coverage width was reduced.

REFERENCES

[1] Krishna, K., Ricklick, M., Heat Transfer Analysis of Jet Impingement Cooling on a Simulated Ceramic Matrix Composite Surface, Proceedings of ASME Turbo Expo 2017, GT2017-64991

[2] Wilkins, P., Lynch, S., Thole, K., Vincent, T., Quach, S., Mongillo, D., Effect of a Ceramic Matrix Composite Surface on Film Cooling, Journal of Turbomachinery, Vol. 144, 2022

[3] Wilkins, P., Lynch, S., Thole, K., Quach, S., Vincent, T., Experimental Heat Transfer and Boundary Layer Measurements on a Ceramic Matrix Composite Surface, Proceedings of ASME Turbo Expo 2020, GT2020-15053

[4] Edelson, R., Thole, K., Impact of Ceramic Matrix Composite Topology on Overall Effectiveness, Journal of Turbomachinery, Vol. 145, 2023

[5] Wilkins, P., Lynch, S., Thole, K., Vincent, T., Quach, S., Kaufman, E., Experimental Investigation Into the Effect of a Ceramic Matrix Composite Surface on Film Cooling, Journal of Turbomachinery, Vol. 144, 2022

[6] Zhao, C., Tu, Z., Mao, J., Investigation of the Film-Cooling Performance of 2.5D Braided Ceramic Matrix Composite Plates with Preformed Hole, Aerospace, Vol. 116, 2021

[7] Boyle, R., Parikh, A., Halbig, M., Nagpal, V., Design Considerations for Ceramic Matrix Composite Vanes for High Pressure Turbine Applications, Proceedings of ASME Turbo Expo 2013, GT2013-95104

[8] Boyle, R., Parikh, A., Nagpal, V., Design Concepts for Cooled Ceramic Composite Turbine Vane, NASA/CR—2015-218390

[9] Smith, C., Presby, M., Bhatt, R., Kalluri, S., the Effects of Cooling Holes on SiC/SiC CMC Tensile Strength, Proceedings of ASME Turbo Expo 2020, GT2020-15682

[10] Mehta, J., Brown, G., Zhong, F., Shouse, D., Neuroth, C., Marshall, D., Cox, B., Multi-hole Film Cooling with Integrally Woven SiC-SiC Ceramic Wall Panels, Proceeding of HT2005, HT 2005-72037

[11] El-Gabry, L., Kaminski, D., Experimental Investigation of Local Heat Transfer Distribution on Smooth and Roughened Surfaces Under an Array of Angled Impinging Jets, Transactions of the ASME, Vol. 127, 2005

[12] Poinsatte, P., Thurman, D., Lucci, B., Detailed Velocity, Temperature, and Heat Flux Measurements on a Large Scale Film Cooling Model, NASA/TM-20220004085, 2022